# CHAOTIC MIXING IN THREE-DIMENSIONAL MICRO CHANNEL

T.H.V. Le,*[1] S. Kang,[2] Y.K. Suh[3] and Y. Wang[1]

# 삼차원 마이크로 채널 내 카오스 혼합

레 뛰 홍 반,*[1] 강 상 모,[2] 서 용 권,[3] 왕 양 양[1]

*The quality of chaotic mixing in three-dimensional micro channel flow has been numerically studied using Fractional-step method (FSM) and particle tracking techniques such as Poincaré section and Lyapunov exponents. The flow was driven by pressure distribution and the chaotic mixing was generated by applying alternating current to electrodes embedded on the bottom wall at a first half period and on the top wall at a second half period. The equations governing the velocity and concentration distributions were solved using FSM based on Finite Volume approach. Results showed that the mixing quality depended significantly on the modulation period. The modulation period for the best mixing performance was determined based on the mixing index for various initial conditions of concentration distribution. The optimal values of modulation period obtained by the particle tracking techniques were compared with those from the solution of concentration distribution equation using FSM and CFX software and the comparison showed their good match.*

**Key Words** : Chaotic Mixing, Poincaré section, Lyapunov exponent, Modulation period

## 1. INTRODUCTION

There has been a recently developing surge of fundamental properties of the mixing due to its application in manufacturing, food, pharmacology and other industries. Obtaining fluid mixing in micro-scales is quite difficult because of absence of turbulence. Flow inside micro channel corresponding with small Reynolds number is always laminar so diffusive mixing will be dominant. Many researches, such as Qian and Bau [13], Lee Y K [12] and etc, recently have based on chaotic advection which promotes the rapid stretching and folding of fluid to enhance fluid mixing within micro channel. In our problem, we have investigated chaotic advection in a pressure distribution driven micro channel. Chaotic mixing is induced by applying alternating current to electrodes embedded on the bottom wall at a first half period and on the top wall at a second half period, respectively. That means, with respect to one specified period, we continuously switched on and off two flow fields at every half periods. Depending on the magnitude and the sign of the zeta potential, a non-uniform slip-velocity which caused chaotic motion generated on the surface at top and bottom walls. The mixing pattern would be different if we adjusted value of modulation period.

## 2. FLOW MODEL AND NUMERICAL METHODS

### 2.1 MATHEMATICAL MODEL

We considered the unsteady and periodic three-dimensional motion of an incompressible fluid within a micro channel which is driven by pressure distribution. In

1 학생회원, 동아대학교 대학원 기계공학과
2 정회원, 동아대학교 기계공학과 교수
3 정회원, 동아대학교 기계공학과 교수
* Corresponding author, E-mail: wook@kari.re.kr

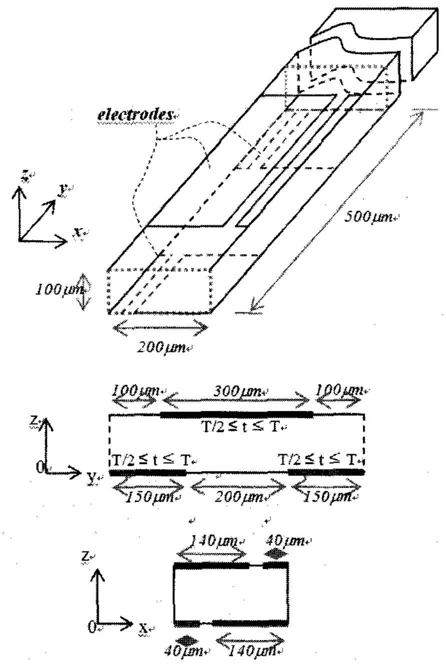


Fig.1 Geometry of the 3D-micorchannel

one period, the two electrodes are mounted along the bottom wall near the inlet and outlet at first half period while another electrode is embedded on top wall at second half period as shown in Figure 1. This generates the non-uniform slip velocity at the walls of micro channel. The governing equations for this problem are written in a dimensionless form as follows

$$\nabla \cdot \mathrm{u_i} = 0, \tag{1}$$

$$\frac{\partial \mathrm{u_i}}{\partial \mathrm{t}} + \mathrm{u_i} \cdot \nabla \mathrm{u_i} = -\nabla \mathrm{p} + \frac{1}{\mathrm{Re}} \nabla^2 \mathrm{u_i}, \tag{2}$$

$$\frac{\partial \mathrm{c}}{\partial \mathrm{t}} + \mathrm{u_i} \cdot \nabla \mathrm{c} = \frac{1}{\mathrm{Pe}} \nabla^2 \mathrm{c} \tag{3}$$

where $u_i = (u, v, w)$ are three non-dimensional velocity components, c is the concentration distribution, $Re(= U_S^* H/\nu)$ is the Reynolds number $Pe(= U_S^* H/D)$ and is the Peclet number; w = W/H = 2, h = H/H = 1 and l = L/H = 5 are the non-dimensionless of micro channel , H is the characteristic length, $U_S^* = 2000\mu m/s$ is the average velocity, D is the diffusive coefficient of concentration distribution, $\nu$ is the kinematical viscosity and $t(= H/U_S^*)$ is the non-dimensionless time. The boundary conditions for velocity field and concentration are:

▣ At the inlet and outlet

$u_{i,outlet} = u_{i,inlet}$, $c_{i,outlet} = c_{i,inlet}$

▣ At the side walls

Velocities: No-slip condition $u_i = 0$

Concentration: zero-gradient condition $\frac{\partial c}{\partial x} = 0$

▣ At the top and bottom walls:

Velocities: Slip condition

Concentration: zero-gradient condition $\frac{\partial c}{\partial z} = 0$

## 2.2 Fractional-Step Method (FSM)

Mixing performance was obtained by solving equations of velocity components and concentration distribution using FSM. The continuity equation is satisfied at each computational time step by a pseudo-pressure which is used to correct the velocity field. In this case, we used a third-order Runge-Kutta method (RK3) for convection term and a second-order Crank-Nicolson method for the diffusion term[7]. Therefore the governing equations will turn to these new equations as follows

$$\frac{\hat{u}_i^k - u_i^{k-1}}{\Delta t} = \alpha_k L(\hat{u}_i^k) + \alpha_k L(\hat{u}_i^{k-1}) - 2\alpha_k \frac{\partial p^{k-1}}{\partial x_i} - \gamma_k N(u_i^{k-1}) - \rho_k N(u_i^{k-2}) \tag{4}$$

$$\frac{\partial^2 \phi^k}{\partial x_i \partial x_i} = \frac{1}{2\alpha_k \Delta t} \frac{\partial \hat{u}_i^k}{\partial x_i} \tag{5}$$

$$u_i^k = \hat{u}_i^k - 2\alpha_k \Delta t \frac{\partial \phi^k}{\partial x_i} \tag{6}$$

$$p^k = p^{k-1} + \phi^k - \frac{\alpha_k \Delta t}{Re} \frac{\partial^2 \phi^k}{\partial x_j \partial x_j} \tag{7}$$

Where $L(u_i) = \frac{1}{Re} \frac{{}^2 u_i}{x_j x_j}, N \cdot \frac{{}^2 u_i}{x_j x_j}, N(u_i) = \frac{u_i u_j}{x_j}$

$\hat{u}_i$ is the intermediate velocity, $\varphi$ is the pseudo-pressure, $\nabla t$ and k are the computational time step and substep's index, and $\alpha_k$, $\gamma_k$ and $\rho_k$ are the coefficients of RK3 ($\alpha_1$= 4/15, $\Upsilon_1$=8/15, $\rho_1$=0; $\alpha_2$=1/15, $\Upsilon_2$=5/12, $\rho_1$=-17/60; $\alpha_3$=1/6, $\Upsilon_3$=3/4, $\rho_3$=-5/12).

The ADI method (Alternating Direction Implicit method) and ICCG method (Incomplete Cholesky Conjugate Gradient method) were used to get the solutions of velocity and pseudo-pressure, respectively.

Mixing index is defined by the following equation

$$D = \sqrt{\frac{1}{N}\sum_{i,j,k}^{N}\left(1 - C_{i,j,k}/\overline{C}\right)} \tag{7}$$

where $c_{i,j,k}$ is concentration at position (i, j, k) in the computation domain, $\overline{c}$: the average concentration at all nodes and N is the total number of nodes in the grid system.

### 2.3 Poincaré Section Analysis

Poincaré section is a graphical analysis tool to capture interesting features such as mixing zones in micro channel flow. Otherwise, it is also a surface in the phase space that cuts across the flow of a given system. The mixing is good when the particles are distributed uniformly in calculation domain after certain periods. With a three-dimensional flow in micro channel, the trajectory or path-line of a fluid as follows

$$\frac{dx}{dt} = u(x,y,z,t), \frac{dy}{dt} = v(x,y,z,t), \text{ and}$$
$$\frac{dz}{dt} = w(x,y,z,t) \tag{8}$$

The positions of a particle in calculation domain are advanced by 4th order Runge-Kutta method.

### 2.4 Lyapunov Exponent Analysis

Lyapunov exponent describes chaotic mixing by determining the position of two initially nearby particles

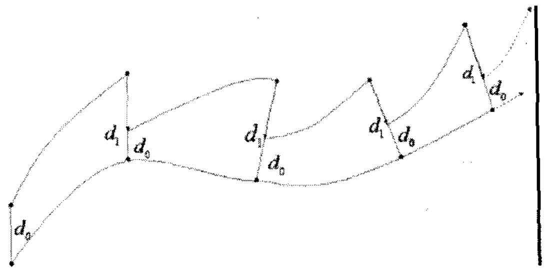


Fig. 2 Schematic for calculation for calculating the Lyapunov exponent.

which will be extremely different after a certain time. The best mixing effect can be obtained when Lyapunov exponent approaches to a maximum value. The largest convergence of Lyapunov exponent should be positive in the chaotic state, when the Lyapunov exponent is calculated by using Sprott's method (Fig. 2) which is manifested by this formula

$$\lambda = \lim_{t\to\infty}\frac{1}{t}\ln\left(\frac{d_i}{d_0}\right) \tag{9}$$

where T is modulation period, $d_0$ is the distance of two near by particles and $d_i$ is next time step's distance of nearby particle and calculated as below

$$d_i = \left[(x_{i+1}-x_i)^2 + (y_{i+1}-y_i)^2 + (z_{i+1}-z_i)^2\right] \tag{10}$$

where the subscripts denote the two orbits, 0 and 1 denoting the virtual and main praticles.

## 3. Results and Discussion

The FORTRAN code was developed for the chaotic mixing in micro channel. The dimensionless of channel (one period) are 2x5x1 in x, y and z directions, respectively. The others parameters were inputted in code is the number of grids 81x141x51 selected by grid convergence test with the fixed Reynolds number Re = 0.2. The mixing process is attained in whole domain of micro channel after total time t = 50 with respect to Pe =

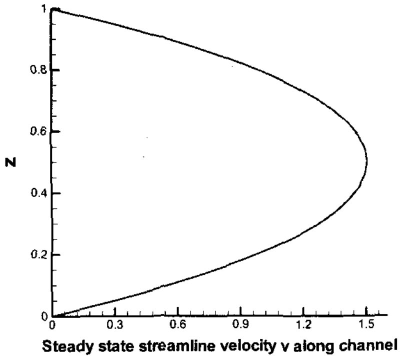


Fig. 3 Steady state downstream velocity v in center plane(y,z) along the micro channel length.

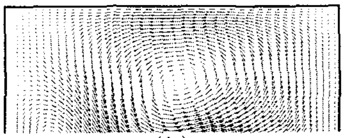

(4a)

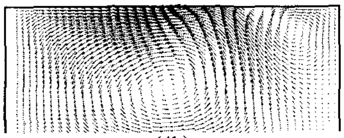

(4b)

Fig. 4 Velocity profile of cross section located at y = 1.25 in first half period (a), and at y = 3.25 in second half period (b).

2000 and Pe = 10,000. For results corresponding witheach Peclet number, the mixing effect is obtained at the six values of modulation periods 0.5, 2, 5, 10, 15 and 20.

Table 1 Mixing index after t=50s with respect to three ICCD

| Case | VS | | HS | | DS | |
|---|---|---|---|---|---|---|
| Pe / T | 2000 | 10000 | 2000 | 10000 | 2000 | 10000 |
| 0.5 | 0.0901 | 0.2821 | 0.1027 | 0.3432 | 0.0913 | 0.2495 |
| 2 | 0.0708 | 0.2581 | 0.0827 | 0.3072 | 0.0762 | 0.2291 |
| 5 | 0.0605 | 0.2368 | 0.0779 | 0.2992 | 0.0659 | 0.2112 |
| 10 | 0.0361 | 0.1469 | 0.0724 | 0.2519 | 0.0401 | 0.1334 |
| 15 | 0.0167 | 0.1333 | 0.0660 | 0.2248 | 0.0388 | 0.2579 |
| 20 | 0.0308 | 0.1436 | 0.0683 | 0.2277 | 0.0488 | 0.1069 |

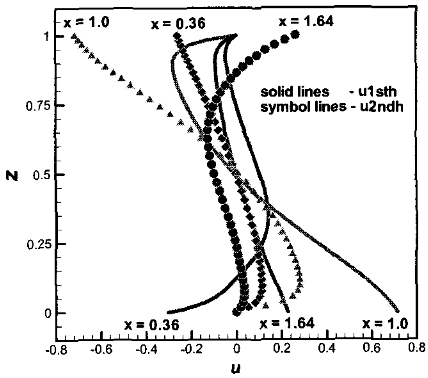


Fig. 5 Steady state velocities u in plane (x,z) located at y=1.25 at first and second half period

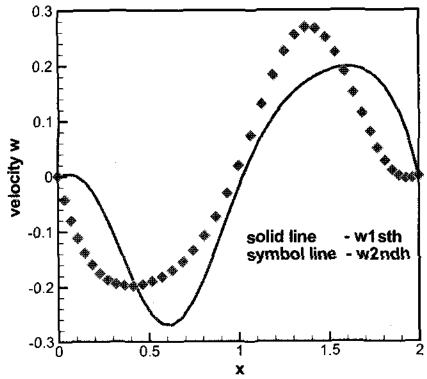


Fig. 6 Steady state velocities w in plane (y,z) located at y = 1.25 at first and second half period

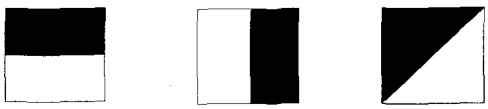

(7a) (7b) (7c)

Fig. 7 ICCD C=1 for black and C=0 for white. (7a) VS – horizontal separation; (b) HS – vertical separation and (c) DS – diagonal separation

### 3.1 Results of Velocity and Mixing Efficiency

Because of a laminar flow in micro channel, the downstream velocity which is dependent on x and z can be solved exactly. By applying a parabolic downstream velocity in whole domain of channel initially, we have got a steady state parabolic velocity v which is zero on the top and bottom wall and maximum in the center, with symmetric distribution (Fig. 3). In plane x-z (y = 1.25), velocity field are symmetric at first and second half

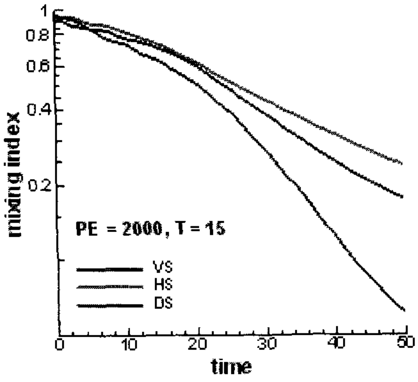


(8a)

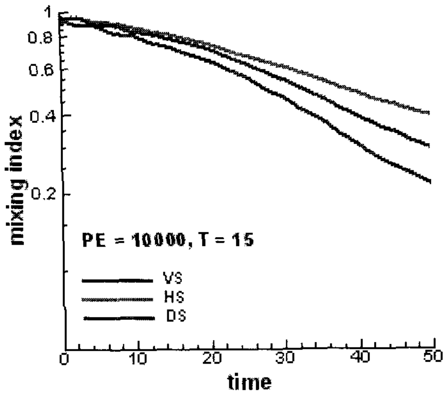


(8a)

Fig.8 Comparison between the lowest value of mixing index.

periods (Fig. 4a and 4b) and similar to the two velocity components u with three positions of x (x = 0.36, x = 1.0 and x = 1.64) and w with position z = 0.5 (Fig. 5 and 6) in plane x-z. The streamlines appear four eddies, two at the bottom wall during first half period and remaining two at the top wall during second half period.

The mixing efficiency was got after t = 50 and the lowest values of mixing index appropriated to initial conditions of the concentration distribution (ICCD), the Peclet number (Pe = 2000 and 10,000) and various modulation periods were showed in table 1. We found that for all ICCD, comparison of mixing index as follows: first, between two values of Peclet number, mixing index with high Pe always bigger than lower Pe. It demonstrates that the same average velocity and dimension of micro channel with high Pe means diffusivity will be very small so that those results in mixing efficiecy is not very good.

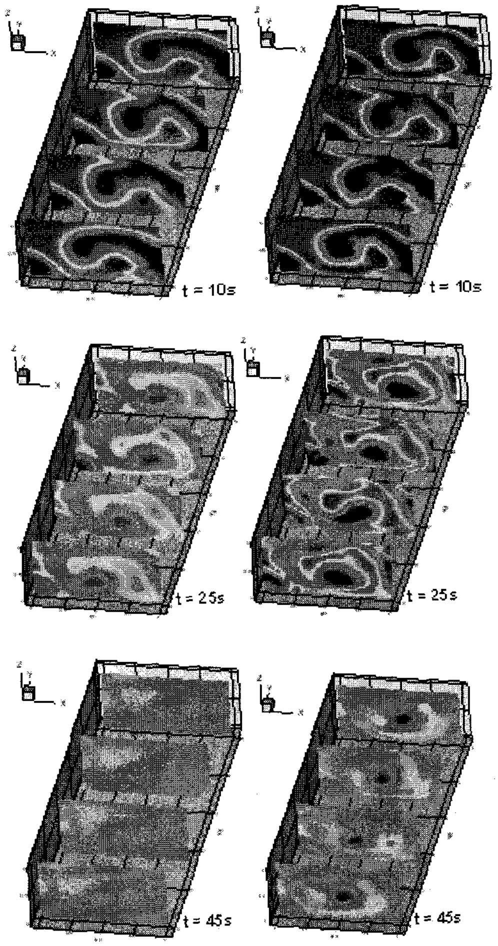


Fig. 9 Mixing performance at different time with Pe= 2000 (left column) and 10,000 (right column)

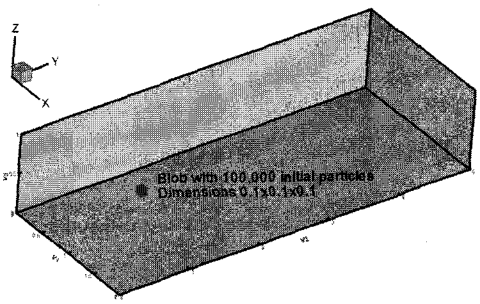


Fig.10 Cubic blob is putted inside the micro channel

Second, between among various modulation periods T, mixing index decreases from T = 0.5-15 and then increases up to 20. That concludes that to get best mixing we must consider suitable value of T. Finally, the best

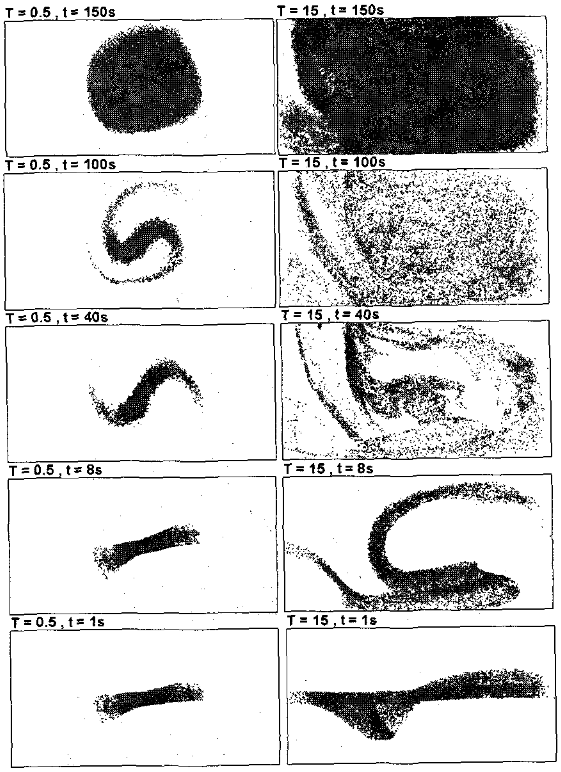


Fig.11 Deformation of a blog at different time with respect to low and high modulation periods T = 0.5 and 15.

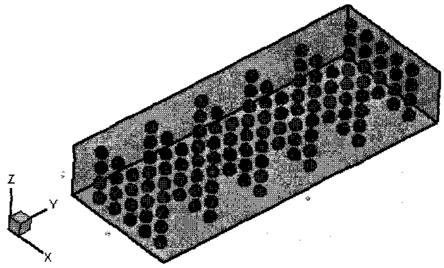


Fig. 12 The initial main particles in calculating domain

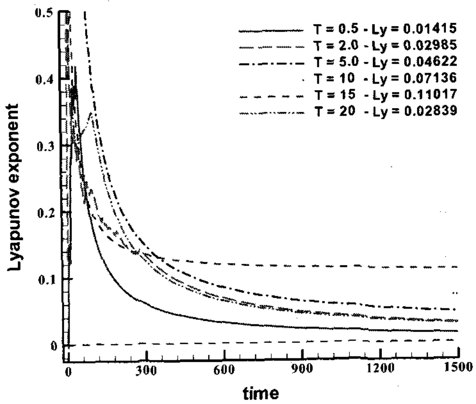


Fig. 13 The convergence of Lyapunov exponent at various modulation periods

mixing were obtained appropriated to ICCD of vertical separation with T = 15 at both of cases of Peclet numbers.

### 3.2 Qualification of Chaotic Mixing Using Poincaré Section

We initially put a cubic blob with 22000 passive particles inside computational domain of channel and observe their motion (Fig 10.). The dimension of blob is 0.1 located at (0.95, 1.2,0.45). We can see that the particles also expand exponentially when time passes and more widely when we increase modulation period. Precisely, at T=2, all particles just move with small distances and finally fixed in small zone. But at high modulation period, the blob is deformed fully and the fluid particles spread to cover almost the entire domain (Fig. 11). The good mixing is achieved at modulation period T = 15. This also show matching value of modulation period when we employed FSM to solve the equation of concentration distribution.

### 3.3 Qualification of Chaotic Mixing Using Lyapunov Exponent

We inputted 120 main particles in micro channel domain and choose 120 virtual particles with each particle is far from main particle d0 = 1.e-5 in the direction z (Fig 12). The largest convergent values of Lyapunov exponent (LE) are obtained with respect to six value of modulation period showed in Fig. 13. We found that LE is increasing corresponding to modulation period increasing. With T=15 LE approached to largest convergent faster then other cases with the value LE = 0.1102. So that means the best mixing qualify can get with respect to value of modulation period T = 15. This also match with the results which we have got using FSM and Poincaré section.

## 4. CONCLUSIONS

We have addressed the chaotic mixing efficiency of the three-dimensional flow within micro channel driven by pressure distribution and the depending-time non-uniform slip velocity on the top and bottom walls. The chaotic mixing is enough good depend on choosing Peclet number and the modulation period, especially in this case is T = 15. By changing in the initial conditions of the concentration distribution considerable also affected mixing performance. The good results of chaotic mixing in this case are to demonstrate FSM is also an advantageous method for simulation of mixing problems. We also showed that the results are matching between using FSM and Particle taking technique (Poincaré section and Lyapunov exponent).

## ACKNOWLEDGEMENT

This study was supported by the Korea Science and Engineering Foundation (KOSEF) through the National Research Laboratory program funded by the Ministry of Science and Technology (No. 2005-01091)

## REFERENCES

[1] 1996, Hardt, S., Drese, K.S., Hseel, V., Schonfeld, F., "Computational Methods for Fluid Dynamics," *Springer*, pp.149-204.

[2] 2000, Patrick D. Anderson, Olesksiy S. Galaktionov, Gerrit W.M. Peters, Frans N. van de Vosse, Han E.H. Meijer, "Chaotic fluid mixing in non-quasi-static time-periodic cavity flows," *Heat and Fluid Flow*, Vol.21, pp.176-185.

[3] 2006, Cerbelli, S., Adrover, A., Creta F. and Giona, M., "Foundations of laminar chaotic mixing and spectral theory of linear operators," *Chemical Engineering Science.*, Vol.61, pp.2754-2761.

[4] 1997, Tatsuo Nishimura and Koji Kunitsugu, "Fluid mixing and mass transfer in two-dimensional cavities with time-periodic lid velocity," *Int. J. Heat and Fluid Flow*, Vol.18, pp.497-506.

[6] 2005, Fredrik Carlsson, Mihir Sen, Lennart Lofdahl, "Fluid mixing induced by vibrating walls," *European Journal of Mechanics B/Fluids*, Vol.24, pp.366-378.

[7] 1999, Galaktionow, O.S., Meleshko, V.V., Peters, G.W.M., Meije, H.E.H., "Stokes flow in a rectangular cavity with a cylinder," *Fluid dynamics Research*, Vol.24, pp.81-102.

[8] 2003, Wang, H., Iovenitti, P., Harvey E. and Masood, Syed., "Numerical investigation of mixing in microchannels with patterned grooves," J. *Micromech. Microeng*, Vol.13, pp.801-808.

[9] Xia, H.M., Shu, C., Wan S.Y.M. and Chew, Y.T., "Influence of the Reynolds number on chaotic mixing in a spatially periodic micromixer and its its characterization using dynamical system techniques," *J. Micromech. Microeng*, Vol.16, pp.53-61.

[10] 2003, Xize Niu and Yi-Kuen Lee, "Efficient spatial-temporal chaotic mixing in microchannels," *J. Micromech. Microeng*, Vol.13, pp.454-462.

[11] 2006, Ducrée, J., Haeberle, S., Brenner, T., Glatzel T. and Zengerle, R., "Patterning of flow and mixing in rotating radial microchannels," *Microfluid Nanofluid*, pp.97-105.

[12] 2001, Lee Y K, Deval J and Tbeling P and Ho C M, "Chaotic mixing in electrokinetically and pressure driven micro flows," P*ro. 14th IEEE Workshop on Micro Electro Mechanical Systems* (IInterlaken, Switzeland, Jan.), pp. 483-486.

[13] 2000, Lui R H, Stremble M A, Sharp K V, Olsen M G, Santiago J G, Adrian R J, Aref H B and David J, "Passive mixing in a three-dimensional serpentine microchannel," *J. MEMS*, Vol.9, pp.190-197.

[14] Qian, S. and Bau, 2005, "Theoretical investigaton of Electroosmotic Flows and Chaotic Stirring in Rectangular Cavities," *Applied Mathematical Modelling*, Vol.29, pp.726-753.